DEVELOPMENT OF A DYNAMIC SIMULATION TOOL FOR THE EXOMARS ROVER

Robert Bauer[(1)], Winnie Leung[(2)], Tim Barfoot[(2)]

[(1)]*Department of Mechanical Engineering, Dalhousie University, Halifax, NS, B3H 1B6, Canada, robert.bauer@dal.ca*
[(2)] *MDA, Brampton, ON, L6S 4J3, Canada,{Winnie.Leung,Tim.Barfoot}@mdacorporation.com*

ABSTRACT

Future planetary missions, including the 2011 European Space Agency (ESA) ExoMars mission, will require rovers to travel further, faster, and over more demanding terrain than has been encountered to date. To improve overall mobility, advances need to be made in autonomous navigation, power collection, and locomotion. In this paper we focus on the locomotion problem and discuss the development of a planetary rover chassis simulation tool that allows us to study key locomotion test cases such as slope climbing in loose soil. We have also constructed rover wheels and obtained experimental data to validate the wheel-soil interaction module. The main conclusion is that to fully validate such a complex simulation, experimental data from a full rover chassis is required. This is a first step in an on-going effort to validate the simulation with experimental data obtained from a full rover prototype.

1. INTRODUCTION

Rovers will continue to be an essential element to future planetary exploration missions. These missions will require rovers to travel over challenging terrain to achieve ambitious scientific objectives. The ability to predict rover locomotion performance is critical during the design, validation, mission planning and operational phases of a planetary robotic mission. Accurate prediction and optimization of rover locomotion performance requires an understanding of the rover multi-body dynamics and corresponding wheel-soil interactions.

Patel *et al.* [1] developed a rover chassis evaluation tool called RMPET which employs wheel-soil analytical models based on Bekker theory [2] and a 3-D simulator for SolidWorks designs. Grand *et al.* [3][4] developed a simulator tool which uses a semi-empirical model to introduce reaction forces between the multi-body dynamics simulator and the soil. In their research, various locomotion modes were simulated including peristaltic locomotion where leg-like degrees-of-freedom (DOF) enabled the suspension to be reconfigured to climb steep slopes. Jain *et al.* [5] and Yen *et al.* [6] describe the development of a virtual rover simulator called ROAMS which can be used for stand-alone simulations, closed-loop simulations with on-board software, or operator-in-the-loop simulations. Although ROAMS employs the Coulomb law for the contact dynamics, current work is focused on replacing this model with more accurate wheel-soil models. Harnisch and Lach [7] describe a simulation tool called Off Road Systems Interactive Simulation (ORSIS) which includes a 3-D multi-body vehicle model, driveline and steering model, tire-soil model and terrain model.

1.1 Motivation

In a Phase A study performed for ESA in 2004, MDA led an international industrial team (Alcatel, Alenia/Laben, Carlo Gavazzi Space and Kayser-Threde) to develop an optimized conceptual design of a rover for the ExoMars Mission. This rover design, shown in Fig. 1, incorporates specialized electrical power generation, thermal control, navigation, telecommunications and vehicle control subsystems.

Carrying a large suite of exobiology instruments, the 240-kg ExoMars Rover will be capable of operating autonomously, traveling several kilometers over rocky Martian terrain, and drilling to collect samples for automatic sample analysis in an on-board robotic laboratory. Planned for launch in 2011, the main purpose of the ExoMars mission is to search for signs of past and present life on Mars.

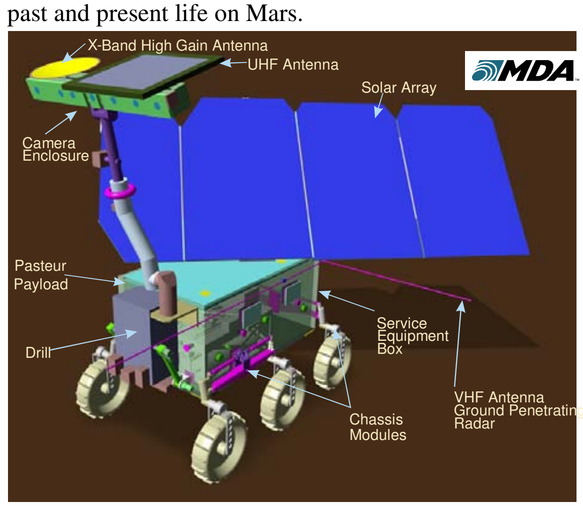

Fig. 1. ExoMars Rover designed by MDA-led team

The mission is highly dependent on a chassis design offering a high degree of mobility to reach the areas of interests on Mars. Locomotion-specific requirements allowing the rover to meet the scientific objectives include the following capabilities:

Proc. of 'The 8th International Symposium on Artifical Intelligence, Robotics and Automation in Space - iSAIRAS', Munich, Germany. 5-8 September 2005, (ESA SP-603, August 2005)

- travel between sampling locations that are 0.5 to 2 km apart
- negotiate rough terrain autonomously, with a range of rock distributions
- drive uphill, downhill and crosshill on loose sandy slopes of 25 degrees
- surmount obstacles that are 0.3 m high
- travel at a maximum speed of at least 100m/h for short duration recovery situations
- point-turn and body posture averaging

Planetary missions such as the ExoMars mission present clear challenges to chassis development and efficient validation of mobility performance. Prototyping is effective but is often too costly and time-consuming to allow multiple iterations within the early design phases. Prototypes also lack the flexibility to provide the opportunity for parametric study of design details. Furthermore, it is difficult to reproduce Martian conditions on Earth.

RCAST presents a well-rounded solution to evaluate rover chassis designs through simulation of mobility performances containing the following features:

- 3-D simulation of multi-body dynamics for complex rigid body systems
- rapid modelling of intricate rover suspensions including representative mass distributions from CAD
- experimentally validated wheel-soil module which takes into account effects of wheel grousers, bulldozing resistance, multipass (wherein the front wheels create a track that the rear wheels follow), and the dependencies between lateral and longitudinal forces
- coupling of low-level control elements with motor and gearbox models, which allows integration of advanced control techniques such as slip optimization
- 3-D visualization of the simulation in a VRML environment

A similar tool, Rover Chassis Evaluation Tool (RCET) from ESA, was not yet available at the time of the Phase A ExoMars Rover-Pasteur study. RCAST was, therefore, developed to characterize and optimize the ExoMars Rover mobility in support of the evaluation of locomotion subsystem designs in the study.

2.0 RCAST ARCHITECTURE

Fig. 2 summarizes the RCAST architecture where the rover multi-body dynamics is based on a rigid multi-body dynamics engine available in Matlab and Simulink's SimMechanics Toolbox [8]. SimMechanics is capable of modelling a large number of DOF and constraints within the Simulink block-diagram environment. SimMechanics, therefore, provides a seamless connection to wide array of Matlab and Simulink toolboxes including the Control System Toolbox which can be used to model the control systems for the rover actuators and sensors.

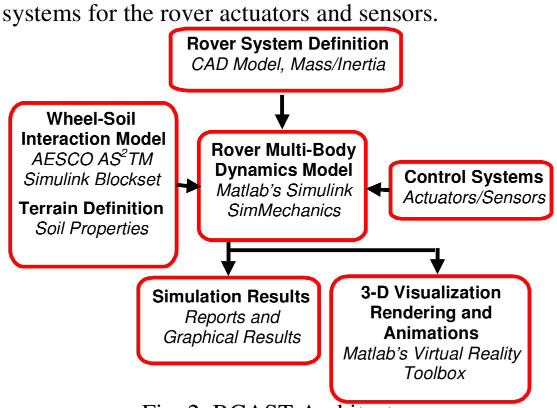

Fig. 2. RCAST Architecture.

CAD models exported from such tools as SolidWorks and ProEng. can be imported into SimMechanics providing a relatively straightforward solution to simulate complex 3-D multi-body rover designs. These CAD models can also be used in conjunction with Matlab and Simulink's Virtual Reality Toolbox which enables the creation of 3D-rendered visualizations and animations of the rover motion [9]. To model the wheel-soil interaction, RCAST uses a commercially-available software package called AESCO Soft Soil Tire Model (AS^2TM)[10].

2.1 Wheel-Soil Interaction Model

AS^2TM can be seamlessly integrated into the Simulink block-diagram environment with an S-Function block. This model further develops the traditional analytical methods which are based on the principles introduced by Bekker [2] and Wong [11]. The vertical and horizontal deformations in the wheel-soil interaction are separated and described by pressure-sinkage and shear-stress to shear-deformation characteristics.

The pressure-sinkage relationship, as proposed by Bekker [2], is described as:

$$p = \left(\frac{k_c}{b} + k_\varphi \right) z^n \quad (1)$$

where p is the pressure, b is the smaller dimension of the contact path/width of the rectangular contact area, z is the sinkage, and n, k_c and k_φ are the pressure-sinkage parameters. The parameter n is called the exponent of sinkage while k_c and k_φ are called the cohesive and frictional moduli of deformation, respectively. The maximum shear stress can be described by either the Coulomb rule:

$$\tau_{\max} = c + p\tan(\varphi) \qquad (2)$$

or by adhesion between the wheel and the soil as follows:

$$\tau_{\max} = p\mu \qquad (3)$$

where c is the cohesion of the soil, φ represents the internal friction angle of the soil, and μ is the friction coefficient. AS^{2}TM chooses the minimum between the adhesion and the internal soil friction to calculate the maximum shear stress[10].

The shear-stress to shear-deformation relationship, as proposed by Janosi and Hanamoto [12], is described by

$$\tau = \tau_{\max}\left(1 - e^{-\frac{j}{K}}\right) \qquad (4)$$

where τ is the shear stress, j is the shear deformation, and K is the tangent modulus of horizontal shear deformation (or slip coefficient).

In order to model the rigid wheels used in this research, AESCO added a new rigid wheel option to AS^{2}TM. With this option the local pressure and local shear displacement under a rigid wheel is used to compute the local stress. Integrating the local shear stress over the contact area provides the lateral and longitudinal forces, while integrating the local pressure (i.e. normal stress) along the contact area provides the vertical reaction force.

For a rigid wheel, the rolling resistance is a result of plastic soil deformation as well as slip sinkage. AS^{2}TM accounts for the tire tread by considering the grouser height and ratio between positive and negative portions of the tread.

2.2 Rover Model Development

The suspension design proposed for the ExoMars rover consists of 6-wheels with the suspension configuration shown in the left-hand side of Fig. 3. This design is based on a chassis concept described in an RCL report for the ESA Aurora Programme ExoMars Mission [13] which has passive DOF associated with the suspension linkages. Additional DOF are associated with the wheels and wheel supports as follows:

- steering DOF on the front two and rear two wheels
- wheel-walking DOF
- wheel-rotational DOF about the wheel axles

These steering, walking, and wheel-rotational DOF are shown in the right-hand side of Fig. 3. Note that an additional 6 DOF are associated with the position and orientation of the rover as it moves.

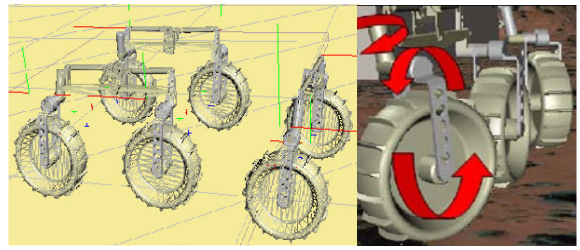

Fig. 3. ExoMars Rover Suspension Configuration

Fig. 4 shows a sample screenshot of the 3-D visualization capabilities of the simulator.

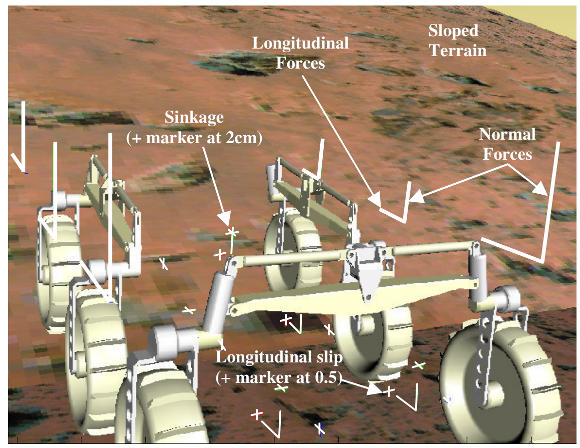

Fig. 4. Sample Screenshot of 3-D Visualization

Note that options have been introduced to enable visualization of the normal, longitudinal and lateral contact forces, as well as the slip ratio and the amount of sinkage during a simulation. The slip ratio is defined as:

$$i = 1 - \frac{v}{\omega r} \qquad (5)$$

where v is the component of wheel carrier velocity in the horizontal direction, ω is the wheel rotational speed, and r is the wheel radius.

2.3 Applications of RCAST

To support rover chassis design and optimization, RCAST is being developed to study various scenarios including slope climbing. In particular, it is desired to determine the ability of various rover designs to negotiate a slope by actuating all six wheel motors and driving straight up the slope, as well as by using additional degrees of freedom on the rover to “walk” the rover up steep slopes.

When driving up a slope, the wheels begin to slip on the soil and the tread causes the wheels to dig into the soil. AS^{2}TM models this slip-sinkage effect and a sample screenshot of this effect is shown in Fig. 5. The slip-sinkage effect leads to a significantly higher rolling resistance which can inhibit the rover's ability to successfully negotiate steep slopes.

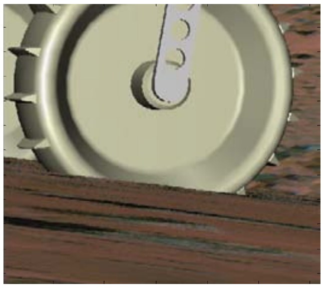

Fig.5. Visualization of Slip-Sinkage Effect

To help overcome this issue, wheel walking can be employed to further extend the rover's slope-climbing ability. Wheel walking is a form of peristaltic locomotion where additional DOF are used to pivot and drive individual wheels forward while locking all other wheels during the maneuver. When implementing wheel walking, there are a variety of wheel-walking sequences that can be implemented with the current ExoMars design. Table 1 and Fig. 6 show one approach to wheel walking where 4 wheel-walking DOF are employed. In Table 1, the front two wheels are referred to as Left 2 and Right 2 where left and right are relative to a viewpoint looking in the direction of forward motion. Left 1 and Right 1 correspond to the middle wheels, and Rear 1 and Rear 2 correspond to the left and right rear wheels, respectively. There are 4 stages to this wheel-walking sequence which are repeated continuously.

In Table 1 there are several wheel control modes which are used throughout the walking sequence. For example, to achieve the configuration shown in the upper-left corner of Fig. 6 (stage 1), the body is pivoted forward by pivoting the forks that support the wheels backward. During this stage it is desired to keep the wheels stationary with respect to the ground. To achieve this motion, the wheels need to be actuated so that the angular motion of the wheel with respect to the fork is opposite to the angular motion of the fork with respect to the ground. The "opposite fork rotation" caption in Table 1 describes this particular wheel control mode. Another wheel control mode is the rolling constraint which is employed in, for example, stage 2 where the front wheels are pivoted forward while keeping all other wheels locked (no rotation). When the wheels are pivoted forward, the commanded angular velocity is that which ensures a rolling constraint where the tangential speed of the wheel is equal to the longitudinal speed of the wheel's axle.

To demonstrate the advantages of wheel walking, simulations were carried out using two different sets of soil parameters corresponding to cloddy and mixed drift-cloddy soil conditions. Table 2 summarizes some example soil properties for these cases as well as some simulation results.

Table 1: Example Schedule of Events for Wheel

		Stage 1		**Stage 2**		**Stage 3**		**Stage 4**	
Wheel	**TimeLine (sec):**	**0**	**5**	**5**	**10**	**10**	**15**	**15**	**20**
Left 2	Walking DOF (deg)	0	-45	-45	45	45	45	45	-45
	Wheel Rotation	opposite fork rotation		rolling constraint		no rotation		opposite fork rotation	
Right 2	Walking DOF (deg)	0	-45	-45	45	45	45	45	-45
	Wheel Rotation	opposite fork rotation		rolling constraint		no rotation		opposite fork rotation	
Left 1	Walking DOF (deg)								
	Wheel Rotation	rolling constraint		no rotation		no rotation		rolling constraint	
Right 1	Walking DOF (deg)								
	Wheel Rotation	rolling constraint		no rotation		no rotation		rolling constraint	
Rear 1	Walking DOF (deg)	0	-45	-45	-45	-45	45	45	-45
	Wheel Rotation	opposite fork rotation		no rotation		rolling constraint		opposite fork rotation	
Rear 2	Walking DOF (deg)	0	-45	-45	-45	-45	45	45	-45
	Wheel Rotation	opposite fork rotation		no rotation		rolling constraint		opposite fork rotation	

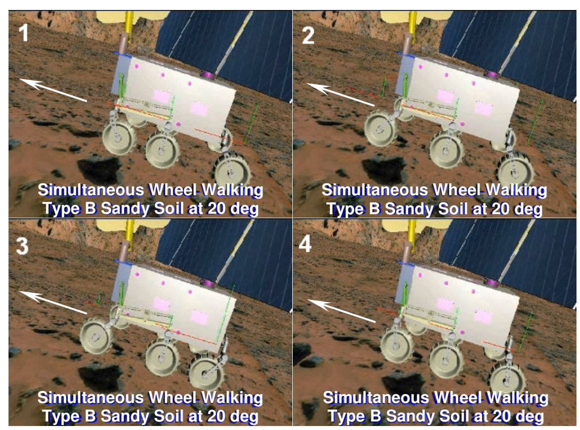

Fig. 6. Example Wheel-Walking Sequence

The simulation results show that wheel walking can enable the rover to climb slopes which are significantly steeper than that achieved by actuating all wheel motors and attempting to drive straight up a slope.

It should be noted that while these results clearly demonstrate that RCAST has the ability to simulate wheel walking to improve slope-climbing ability, the results are subject to change because, in addition to the parameters presented in Table 2, several AS^2TM soil- and tire-related parameters have not yet been finalized through experimentation. These soil parameters are discussed further in the following section where experimental data from a single-wheel testbed is used as first step towards validating and calibrating the 6-wheeled rover in RCAST.

Table 2: Soil Properties in RCAST and Results for Slope Climbing simulations

Soil Parameter	Cloddy	Mixed Drift-Cloddy
ρ	1.55 g/cm^3	1.35 g/cm^3
n	1	1
k_c	0.14 N/cm$^{(n+1)}$	0.14 N/cm$^{(n+1)}$
k_φ	0.82 N/cm$^{(n+2)}$	0.82 N/cm$^{(n+2)}$
K	1.6 cm	1.6 cm
φ	37°	33.1°
c	0.017 N/cm^2	0.022 N/cm^2
Results of Slope-Climbing Case in RCAST		
maximum slope without wheel walking	18°	16°
maximum slope with wheel walking	25°	23°

3. EXPERIMENTAL VALIDATION

In order to validate the simulation results, wheel-soil interaction experiments were carried out on a wheel-terrain characterization testbed and the results were compared with a single-wheel dynamic computer simulator which was developed in Matlab and Simulink's SimMechanics toolbox using AS^{2}TM [14].

3.1 Wheels Tested

A cylindrical wheel was tested in this research. This wheel was designed so that the number of grousers or lugs on the wheel could be easily changed from 9 to 18 by attaching different plates to the surface of the wheel. Fig. 7 shows the two grouser configurations used in this research.

Fig. 7. Cylindrical Wheel with 9 and 18 grouser plates attached

3.2 Experimental Apparatus

To validate the wheel-soil interaction model using these two wheel treads, experiments were performed on the Massachusetts Institute of Technology (MIT) Field and Space Robotics Laboratory's Wheel-Terrain Characterization Testbed as shown in Fig. 8. This testbed consists of a wheel carriage which is equipped with potentiometers and which can translate both horizontally and vertically. A torque sensor and motor are attached to the wheel and a force/torque transducer is located on the wheel carriage above the wheel. Controlling the translational velocity of the wheel carriage and the angular velocity of the wheel enables one to control the slip ratio which is defined in Eq. 5.

With this setup, the wheel-soil interaction forces and torques as a function of slip ratio can be measured. The directions for positive sensor force and torques are superimposed in Fig. 8 and forward motion corresponds to the wheel moving to the left of this figure.

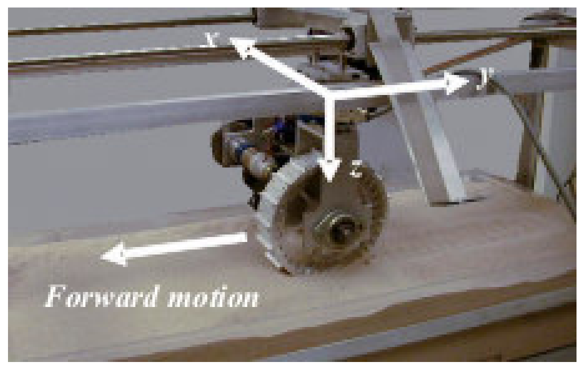

Fig. 8. Wheel-Terrain Characterization Testbed at MIT's Field and Space Robotics Laboratory

A dry sandy soil was used in the testbed and a series of experiments were conducted to characterize the soil parameters. Soil density ρ was measured using an electronic balance. Flat-plate sinkage experiments, as shown in Fig. 9a) were performed similar to the method described by Bekker [2] and Wong [11] using flat plates constructed to correspond to the size of the test wheel. The results of this analysis provided estimates of the pressure-sinkage parameters n, k_c and k_φ. It should be noted that flat-plate sinkage experiments are normally carried out with an apparatus which allows larger vertical loads than those achievable with the Wheel-Terrain Characterization Testbed. Larger loads would induce higher sinkage measurements and improve the accuracy of the calculated n, k_c and k_φ soil parameters. Alternatively, improving the resolution of the potentiometer used on the testbed to measure sinkage would also likely improve the confidence in the calculated soil parameters.

The shear-deformation modulus K was determined using the apparatus shown in Fig. 9b). The apparatus is similar to those used for the standard direct shear test in Civil engineering where known horizontal displacements are imposed at the interface while the vertical displacement is measured[15]. The internal friction angle φ was determined from the slope of the soil when piled as shown in Fig. 9c).

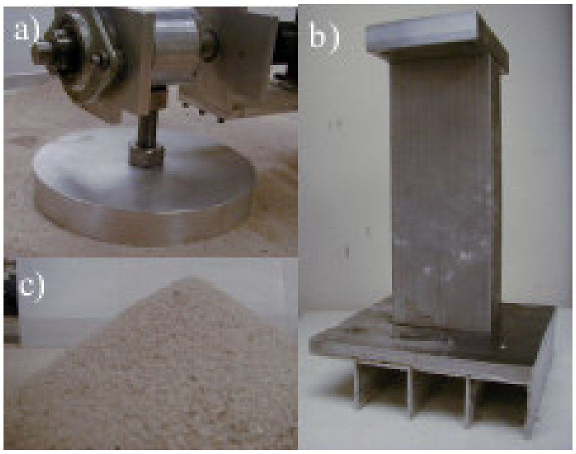

Fig. 9: Characterizing Soil Parameters

Table 3 summarizes the soil parameters measured from these experiments.

Table 3: Measured Soil Parameters

Parameter	*Value*
ρ	1.605 g/cm^3
n	1.1
k_c	0.65 N/cm$^{(n+1)}$
k_φ	3.35 N/cm$^{(n+2)}$
K	1.5 cm
φ	32°

3.3 Experimental Results

For each tire tread, experiments were carried out for the following 7 slip ratios: 0.04, 0.15, 0.24, 0.35, 0.46, 0.57, 0.66. For each slip ratio, at least 3 trials were performed to provide an indication of the repeatability of the experiments. The trials for each experiment were merged into a single dataset and the last two seconds of each merged dataset was averaged to obtain the steady-state mean values. These data were calculated for each of the two tire treads and the experimental results are plotted in Fig. 10 and Fig. 11 as a function of slip ratio.

Fig. 10 shows that the measured sinkage vs. slip-ratio data are very similar for both wheel treads at slip ratios below 0.5. It is evident from Fig. 11 that doubling the number of grousers increases the drawbar pull F_y by approximately 30%. The negative values of the measured sensor forces F_y in Fig. 11 are consistent with the sensor coordinate frames shown in Fig. 8.

4. COMPARING EXPERIMENTAL RESULTS WITH SIMULATION RESULTS

In order to compare the above experimental results with the AS^{2}TM soft-soil tire model, the soil parameters associated with this model need to be tuned.

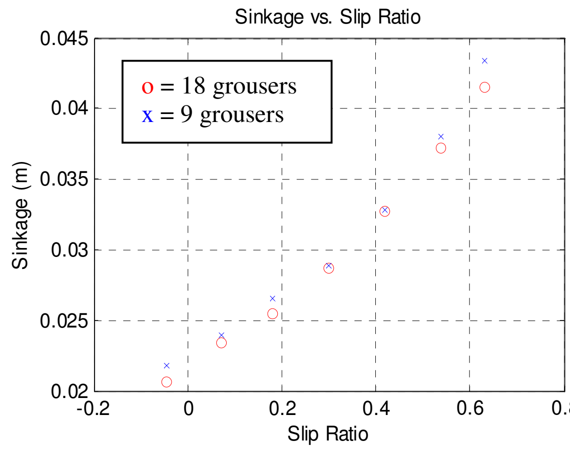

Fig. 10. Sinkage vs. Slip Ratio

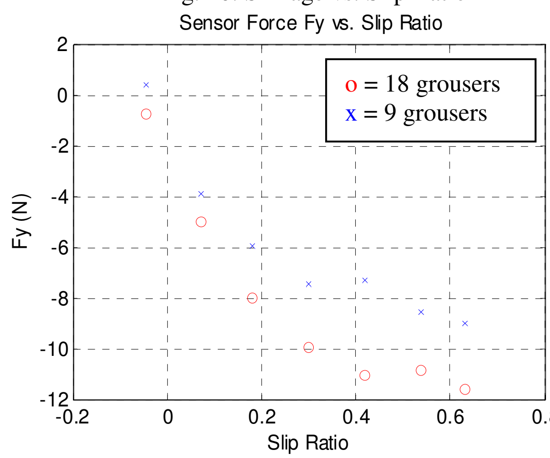

Fig. 11. Drawbar Pull vs. Slip Ratio

4.1 Tuning of Soil Parameters used in the Model

There are several soil parameters used in AS^{2}TM that need to be determined experimentally. These include the density ρ of the soil, n, k_c and k_φ as defined in Eq. 1, the cohesion c, friction angle φ, slip coefficient K, stiffness c_B, damping b, *slippery* (maximum friction coefficient for the surface), *grip* (maximum friction coefficient for the tire), *compaction capability* (used for multipass), *rolling resistance correction* (to account for effects such as bulldozing), and *shear offset* (used for sandy soils). While the first 7 of these soil parameters are traditional Bekker's soil parameters, the remaining parameters are less conventional. c_B, b, *slippery* and *grip* can be estimated through experiments but the last two parameters are considered tuning parameters.

It is challenging to tune these parameters because each parameter often influences more than one measured system response. Based on experience gained by working with the experimental and simulation data, the following tuning approach was developed as part of this research:

1. start with *shear offset=0* and tune k_φ to obtain the correct sinkage at small slip ratios
2. adjust c_B to modify the drawbar pull F_y
3. adjust the *shear offset* so that sinkage predictions agree with experimental results for high slip ratios

During the tuning of these parameters, the following general trends were observed:

- as *rolling resistance correction* increases, *Fy* becomes positive at high slip ratios
- as k_φ increases, the sinkage decreases
- as c_B decreases, sinkage decreases, |*Fy*| increases, and |*Motor Torque*| increases
- as k_c increases, |*Fy*| increases and sinkage decreases
- as *c* increases, |*Fy*| increases and |*Motor Torque*| increases
- increasing the *compaction capability* parameter reduces the subsequent sinkage predictions as wheels repeatedly pass over the track. Note that *compaction capability* only affects multipass cases.

Table 4 summarizes the soil parameters tuned using this procedure on experimental data from the wheel with 18 grousers. The damping *b* was assumed to be very high and the cohesion *c* was assumed to be negligible for the dry sandy soil.

Note that the *compaction capability* parameter was tuned as a last step using multipass experimental data where, after the first pass, the wheel was allowed to pass through its track an additional two times. Also note that AS^2TM uses the smallest value between the *slippery* and *grip* parameters for the friction-related calculations.

Table 4: Tuned Soil Parameters

Parameter	*Value*
ρ	1.605 g/cm^3
n	1.1
k_c	0.65 N/cm$^{(n+1)}$
k_φ	1.80 N/cm$^{(n+2)}$
K	1.5 cm
c	0
φ	32°
b	4000 Ns/m
c_B	1500 N/cm^3
slippery	0.35
grip	1.1
shear offset	0.16 cm
rolling resistance correction	0.05
compaction capability	2.3

4.2 Comparison of Simulation and Experimental Results

Fig. 12 compares the resulting experimental and simulation data as a function of slip ratio for wheel treads with 18 grousers. Note that for each experimental data point, the 95% confidence interval is plotted. Evidently, the sinkage relationship is accurately modeled. The drawbar pull F_y simulation responses fall within the 95% confidence levels, although the predicted increase in drawbar pull above slip ratios of 0.5 is not observed in the measured response which levels off in this range. A leveling off or decrease in the drawbar pull can be explained physically because the increase in horizontal force due to a higher slip ratio is offset by an increase in the rolling resistance due to the higher sinkage of the wheel. The simulation model therefore presents a limit in accurately predicting the rolling resistance due to sinkage at high slip ratio.

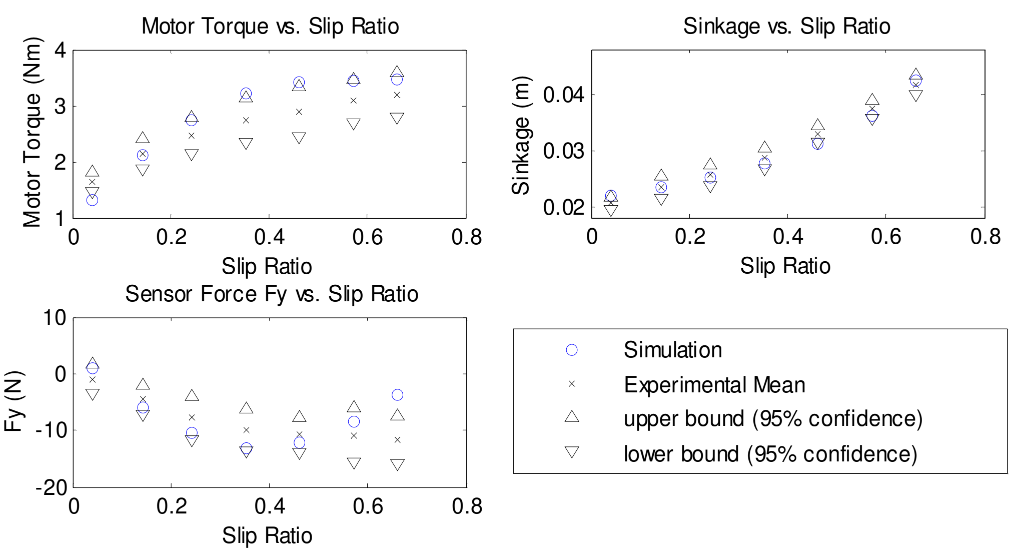

Fig. 12. Simulation and Experimental Data vs. Slip Ratio Measured Sinkage vs. Slip Ratio, 18 grousers

5. CONCLUSIONS

In conclusion, a rover chassis and analysis computer simulation called RCAST has been developed which successfully couples a rigid multi-body dynamics engine with the AS^2TM wheel-soil interaction module to study locomotion performance for various rover designs including the ExoMars rover. Validation of RCAST requires experimental data and, as a first step, single-wheel experiments were carried out for two tire treads, with the measured responses comparing favourably with the estimated responses obtained with the AS^2TM wheel-soil interaction model.

The RCAST tool has been effectively applied to draw some useful conclusions in the conceptual design of the ExoMars Rover. Preliminary simulation results have shown that wheel walking can significantly improve the rover's slope-climbing abilities, with more work needed to validate these results. Experiments showed that, for the dry sandy soil used in this research, the wheel with 18 grousers had approximately 30% improvement in drawbar pull over the wheel with 9 grousers with relatively little effect on sinkage. When comparing these experimental results to simulation results, AS^2TM is able to capture the sinkage vs. slip ratio relationship accurately. More research is required to further study the differences observed in the drawbar pull F_y and motor torque, as well as the ability of AS^2TM to model other scenarios such as side-slip. To fully validate RCAST with all 6 wheels and have confidence in the predictions, experimental data from a full rover chassis will be required. The construction of such an experimental testbed is ongoing work.

6. ACKNOWLEDGEMENTS

The authors would like to thank Dr. Carsten Harnisch and Dr. Björn Lach of AESCO GbR for their support of AS^2TM. The authors would like to thank Professor Steven Dubowsky, Dr. Karl Iagnemma and Dr. Christopher Brooks at MIT's Field and Space Robotics Laboratory for their support of the single-wheel experiments. The authors would also like to thank Steve Fisher at MDA for designing the wheels tested in this research, as well as Robert Carr and Howard Jones at MDA for their support throughout the project.

7. REFERENCES

1. Patel, N., Ellery, A., Allouis, E., Sweeting, M., Richter, L., "Rover Mobility Performance Evaluation Tool (RMPET): A Systematic Tool for Rover Chassis Evaluation via Application of Bekker Theory", 8th *ESA Workshop on Advanced Space Technologies for Robotics and Automation, ASTRA 2004*, ESTEC, Noordwijk, The Netherlands, 2-4 November, 2004, pp. 251-258.
2. Bekker, M., "Introduction to Terrain Vehicle Systems", University of Michigan Press, Ann Arbor, USA, 1969.
3. Grand, Ch., Ben Amar, F., Plumet, F., Bidaud, P., "Simulation and Control of High Mobility Rovers for Rough Terrains Exploration", *Proceedings of the IARP International Workshop on Robots for Humanitarian Demining*, Vienne, Autriche, November 2002, pp. 51-56.
4. Grand, C., Ben Amar, F., Bidaud, P., "A simulation system for behaviour evaluation of off-road mobile robots", *Proceedings of the 4th International Conference on Climbing and Walking Robotics, Karlsruhe*, Germany, September 2001, pp 307-314.
5. Jain., A., Guineau, J., Lim, C., Lincoln, W., Pomerantz, M., Sohl, G., Steele, R., "ROAMS: Planetary Surface Rover Simulation Environment", *Proceedings of the International Symposium on Artificial Intelligence Robotics and Automation in Space (i-SAIRAS)* Nara, Japan, May 19-23, 2003.
6. Yen, J., Jain, A., Balaram, J., "ROAMS: Rover Analysis, Modeling and Simulation", *Proceedings of the International Symposium on Artificial Intelligence Robotics and Automation in Space (i-SAIRAS)*, Noordwijk, The Netherlands, June 1999.
7. Harnisch, C., Lach, B., "Off Road Vehicles in a Dynamic ThreeDimensional Realtime Simulation", *Proceedings of the 14th International Conference of the International Society for Terrain-Vehicle Systems*, Vicksburg, MS, US, October 20-24, 2002.
8. The Mathworks, "SimMechanics Toolbox User's Guide", 2002.
9. The Mathworks, "Virtual Reality Toolbox User's Guide", 2004.
10. AESCO, "Matlab/Simulink Module AESCO Soft Soil Tyre Model (AS^2TM) User's Guide", 2003.
11. Wong, J.Y, "Theory of Ground Vehicles", Third Edition, John Wiley & Sons, Inc., 2001.
12. Janosi, Z. Hanamoto, B., "Analytical Determination of Drawbar Pull as a Function of Slip for Tracked Vehicles in Deformable Soils", *Proceedings of the 1st International Conference on Terrain-Vehicle Systems*, Turin, 1961.
13. Kucherenko, V., Gromov, V., Kazhukalo, I., Bogatcheve, A., Vladykin, S., Manykjan, A., "Engineering Support on Rover Locomotion for ExoMars Rover Phase A, Report 1 – Preliminary Adaptations of Original Concept", RCL Report Ref. Nr. PAOC-1011/2003/RCL, Science & Technology Rover Company Ltd., 2003.
14. Bauer, R., Barfoot, T., Leung, W., "Experimental and Simulation Results of Wheel-Soil Interaction for Planetary Rovers," submitted to IEEE International Conference on Intelligent Robots and Systems 2005.
15. Lambe T.W., Whitman R.V. "Soil Mechanics", John Wiley & Sons, Inc., 1969.